Journal of Sustainable Construction Materials and Technologies
Web page info: https://jscmt.yildiz.edu.tr
DOI: 10.47481/jscmt.1554809

JSCMT
Journal of Sustainable Construction Materials and Technologies

Research Article

Experimental investigation of mechanical and physical properties of glass fiber reinforced concretes produced with different magnetized waters

Serkan SUBAŞI[1], Doğu RAMAZANOĞLU[2], Muhammed MARAŞLI[2], Volkan ÖZDAL[2], Yasemin HATİPOĞLU[2], Heydar DEHGHANPOUR*[3]

[1]*Department of Civil Engineering, Düzce University Faculty of Engineering, Düzce, Türkiye*
[2]*Fibrobeton Company, Department of R&D, Düzce, Türkiye*
[3]*Department of Civil Engineering, İstanbul Aydın University Faculty of Engineering and Architecture, İstanbul, Türkiye*

ARTICLE INFO

Article history
Received: 21 May 2024
Revised: 03 July 2024
Accepted: 30 August 2024

Key words:
Fracture mechanics, GFRC, magnetized water, microstructure, UPV

ABSTRACT

Magnetized water may act as a thickener in cementitious mixtures due to its slippery effect. Therefore, it can be beneficial for the mixture to settle easily and to improve its strength. This study investigated the effects of magnetized water passing through pipes with magnetic field intensity (MFI) 8 and 10 on glass fiber reinforced concrete (GFRC). Three different mixtures, the GFRC mixture produced with regular tap water, were obtained, and the properties of the produced GFRC samples, such as 7, 14, and 28 days H-Leeb hardness, density, Ultrasonic pulse velocity (UPV), flexural strength, compressive strength, and fracture mechanics were investigated. In addition, SEM, EDS, FTIR, and TGA analyses were carried out to investigate the change in surface tension in the internal structures of GFRCs produced with magnetized water. Overall, the results were promising. Results showed a proportional H-Leep hardness increase with curing time and density variations. Magnetized water reduced air voids, enhancing sound transmission speeds. Flexural and compressive strength improved with magnetic water. The study suggests significant contributions to energy savings and reduced production costs, highlighting the efficient use of energy resources.

Cite this article as: Subaşı, S., Ramazanoğlu, D., Maraşlı, M., Özdal, V., Hatipoğlu, Y. & Dehghanpour, H. (2024). Experimental investigation of mechanical and physical properties of glass fiber reinforced concretes produced with different magnetized waters. *J Sustain Const Mater Technol*, 9(3), 280–293.

1. INTRODUCTION

Concrete is a composite with a wide area of use as a building material due to its high compressive strength, hardness, and durability [1]. At the same time, concrete is brittle and weak in tension. Low tensile and tensile strength is the weakest aspect of plain concrete. These deficiencies can be eliminated by retrofitting. Fiber-reinforced concrete (FRC) is a relatively new concrete material made from hydraulic cement, aggregates, and reinforcing fibers. It is a composite containing a dispersion of natural or artificial tiny fibers with high tensile strength. The fibers in its matrix increase the cracking strength of concrete [2]. There is nothing new in this technique, as using fibers in concrete is very ancient [3]. At the beginning of the 20th century, there were developments in the production of glass fibers, mainly of the borosilicate type (E-glass). The first production of Glass Fiber Reinforced Cement dates back to the late 1950s when E-glass fibers were combined with non-alkaline matrices. It was understood then that the al-

***Corresponding author.**
*E-mail address: heydar.dehghanpour@yahoo.com / haydardehgan@aydin.edu.tr

kaline environment of hardened ordinary Portland cement caused corrosion and loss of tensile strength of E-glass fibers. Therefore, Glass fiber reinforced concrete (GRC) production required unusual cement and was very limited. Unique alkaline-resistant glasses were only developed and produced on a commercial scale in the late 1960s [3, 4]. Glass fiber reinforced concrete (GFC) is a material that has contributed significantly to the economy, technology, and aesthetics of the construction industry worldwide for nearly 40 years [5].

Water that is exposed to a magnetic field is called magnetized water. At the end of this exposure, the physical properties of the water change [6]. The main difference between regular water and magnetized water is the hydrogen bonding. In normal water, water molecules behave in clusters that slide over each other, resulting from hydrogen bonding. As the hydrogen bond between these clusters and groups is broken in the water entering the magnetic field, the number of water molecules moving collectively decreases. Thus, the activity of the water increases [7, 8]. Magnetized water's electromagnetic properties, thermodynamic bond angle, dielectric constant, electrical conductivity, pH, solubility, viscosity, surface tension, boiling point, and freezing point differ from normal water [9]. Even if the magnetic field effect disappears, this change in the water shows its impact for a long time [10]. Applying the magnetic field causes a significant increase in the ultraviolet absorption of water. The exposure time of water to the magnetic field increases the absorption intensity of UV rays. In addition, magnetic water, which has a lower surface tension than pure water, turns into a more hydrophilic structure [11].

Surface tension in water is important for concrete's hydration and hardening process. During hydration, cement particles and water molecules react, forming a thin layer, which prevents the reaction from progressing. Because of this inhibition, the cement partially accompanies the reaction. Therefore, the strength values of the cement particles relative to the final concrete cannot be precisely obtained. Using magnetized water instead of regular water in the hydration process of concrete prevents the hydrate residue from forming around the cement particles since the surface tension is lower than regular water, thus allowing more cement to mix with water. Therefore, an improvement is observed in the strength values of the concrete to be formed [11–13].

This study examines the effects on the mechanical and physical parameters of GFRC concretes produced using magnetized water obtained from equipment with two magnetic fields with magnetic field intensity (MFI) of 8 and 10.

2. MATERIALS AND METHODS

2.1. Materials

In this study, Mk37 Silver (1.222 Kg. / 5 cm x 5 cm x 36 cm. / 8 magnetic fields. / 16 magnets) and Mk37 Gold (1.490 Kg. / 5 cm x 5 cm x 45 cm. / 10 magnetic fields. / 20 magnets), which outer surfaces are aluminum anodized and inner surfaces are chrome steel, with a diameter of ¾ inch and a minimum pressure strength of 2 Bar, were used to obtain magnetized water (Fig. 1). CEM II/B-L 42,5R Portland cement was the binder material. Silica sand with a diameter of less than 1 mm was used as filling material, and Calcined kaolin (2.52 g/cm³) was used as pozzolanic. Fibro WR-78 was chosen as the superplasticizer. Alkaline-resistant glass fibers (AR-GF) with a length of 12 mm and a diameter of 14 µm were used as the fiber. The chemical components of cement, calcined kaolin, and silica sand used in GRC production are summarized in Table 1. Sample views of the materials used in the study are shown in Figure 2.

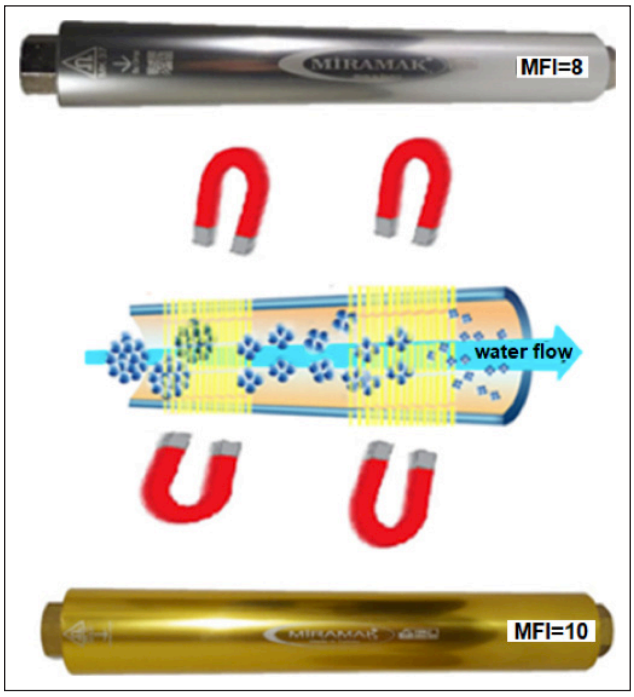

Figure 1. The divergence of water molecules from each other by the effect of the magnetic field.

Table 1. Chemical components of mineral materials used in the construction of GRC

components (wt.%)	Cement	Silica sand	Calcined kaolin
SiO_2	17.46	98.57	59.78
$A1_2O_3$	3.27	0	10.23
Fe_2O_3	0.21	0.17	0.44
CaO	63.04	0.29	9.91
MgO	1.67	0	1.59
K_2O	0.34	0.16	0.9
Na_2O	0.3	0	0.05
SO_3	3.02	0	1.25
P_2O_5	0.04	0.01	0.04
TiO_2	0.09	0.12	0.15
Cr_2O_3	0.0021	0.0137	0.0186
Mn_2O_3	0.0042	0.0029	0.0077
LOI	11	0.39	16.24

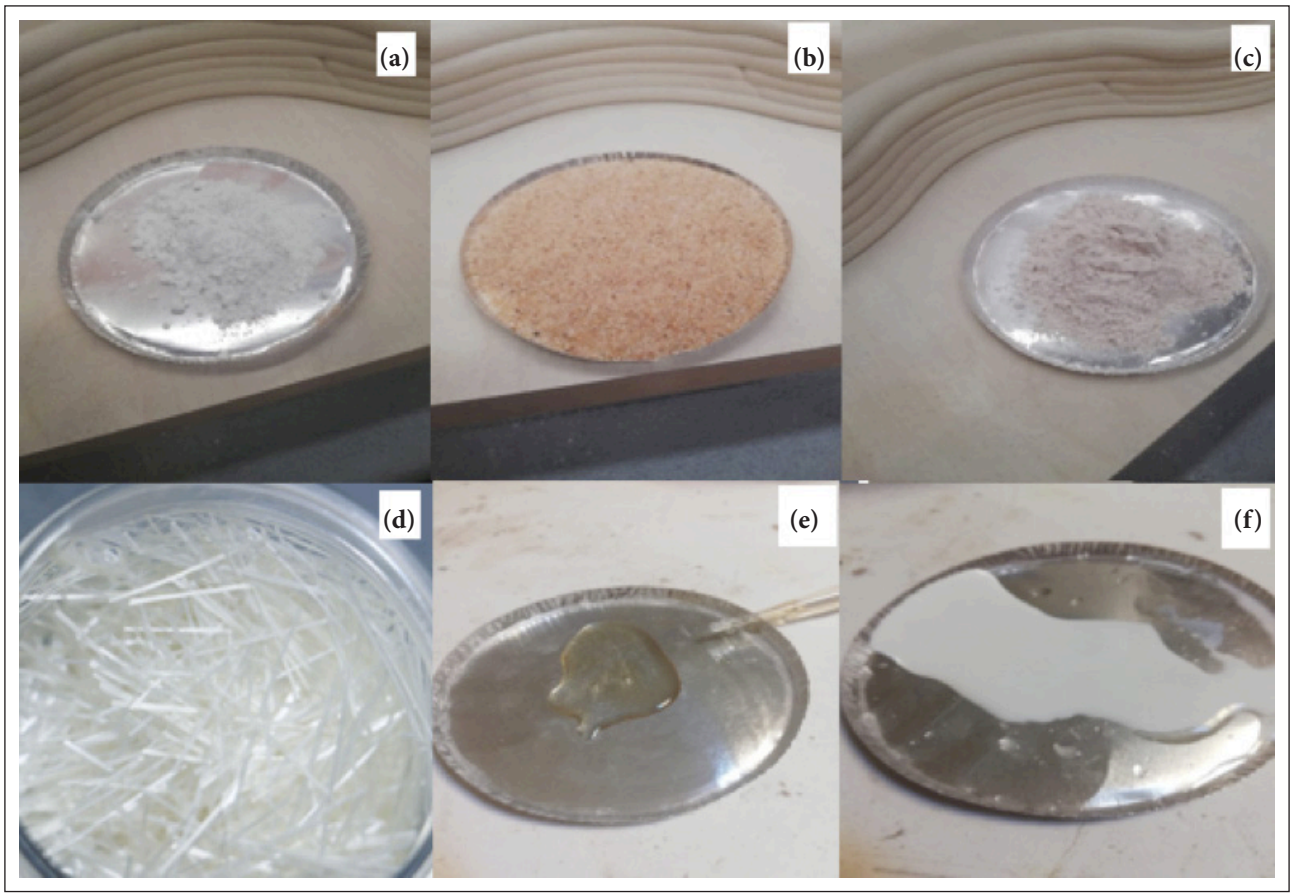

Figure 2. GRC concrete mortar components; CEM II/B-L 42.5R Portland Cement **(a)**, Aggregate/Silica sand **(b)**, Calcined kaolin **(c)**, Alkali resistant glass fibers **(d)**, Plasticizer **(e)** and **(f)** Acrylic polymer.

Table 2. Type and proportions of materials used

No	Material	Type	Amount
1	Cement	Çimsa white 42.5 R	33.75 kg
2	Silica sand	AFS NO: 30–35	37.95 kg
3	Water	Tap water/MFI8/MFI10	12.00 kg
4	Polymer	Betton Bettolatex	1.23 kg
5	Plasticizer	Fibro WR-78	90.00 g
6	Mineral additive	Calcined Kaolin	3.75 kg
7	Fiber	Alkaline-resistant glass fibers 32 mm	3.27 kg

2.2. Method

Spray and premix methods are generally used in GRC production [14, 15]. In this study, the premix method was preferred. The GRC mixture of cement, aggregate, calcined kaolin, and glass fibers was mixed in dry form for about 3 minutes. Then, acrylic polymer, superplasticizer, and magnetized water were added and mixed for 2 minutes. All mixes were produced with a single design component specified in Table 2.

For compressive strength, cube samples of 50 mm^3 were prepared, and their 7, 14, and 28-day strengths were tested according to the TS EN 196-1 standard [16]. Before the compressive strength tests, the density values of the 7, 14, and 28-day-old concrete samples were determined. In addition, Leeb hardness tests of cube samples were carried out according to ASTM-A956 [17]. To determine the flexural strength of the composites, the tests of 270 × 50 × 12 mm samples at 7, 14, and 28 days were carried out according to the TS EN 1170-4 standard [18]. Ultrasonic pulse velocity (UPV) tests were carried out according to ASTM C 597 standard [19] to determine the ultrasonic sound transmission velocity of GRC concrete samples. The morphologies of GFRC samples were analyzed by scanning electron microscopy (SEM) on an FEI model Quanta FEG 250 in secondary electron mode at 10 keV. Fourier Transform Infrared Spektrofotometre (FT-IR) analyses were performed to examine the molecular bond properties of the samples. Thermogravimetric analysis (TGA) and differential scanning calorimetry (DSC) measurements were performed with Shimadzu DTG

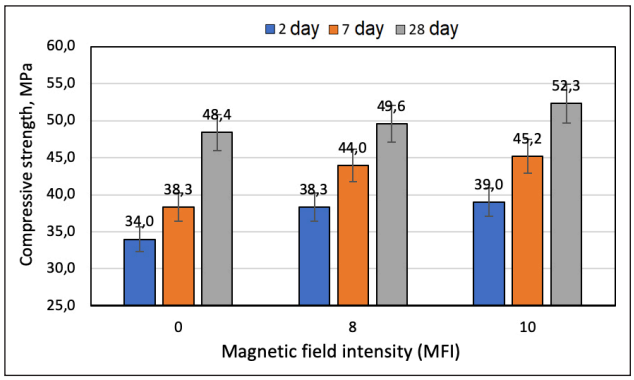

Figure 3. Compressive strengths of GRC composites produced with different magnetic waters.

60H - DSC 60 Thermal Gravimetric Analyzer with high purity nitrogen and 50 mL/min flow rate.

3. RESULTS AND DISCUSSION

3.1. Compressive Strength of GRC Composites

The compressive strengths of GRC concrete prepared with water magnetized in different magnetic fields are given graphically in Figure 3 according to different curing times and magnetized areas. As evident in the graph and other test results, curing periods have positively influenced the compressive strength of concrete, and the use of magnetized water in mortar production is observed to enhance the compressive strength performance of specimens compared to those produced with normal water. The performances at early curing periods, considered as 2 and 7 days, in GRC specimens produced with water exposed to 8 magnetic fields have shown increases of 12.4% and 14.9%, respectively. The ratio of compressive strength performance at 28 days is 2.48%, indicating a relatively lower increase compared to the early ages. In GRC specimens produced with water passing through 10 independent magnetic fields, the compressive strength performances for early periods were 14.7% and 18.0%, and a subsequent increase of 8.05% was observed in the long-term aging at 28 days. An increase in NMF enhances the mechanical strengths of GRC concrete material.

Magnetized water is a type of water that has been treated under the influence of a magnetic field, which organizes the water molecules and changes the physical properties of the water [20]. This water can affect reactions and material properties in the concrete mixture. Various studies [21–24] show that magnetized water can positively affect concrete strength. Magnetized water is thought to help arrange the water molecules in the concrete mixture and hydrate the cement particles more effectively. This can increase the early strength of concrete and improve its overall mechanical properties. However, these effects can vary depending on many factors, so obtaining specific results for each concrete mix and type of magnetized water is essential. The impact of magnetized water on the strength of concrete will depend on a number of factors, including various parameters such as mixing proportions, type of cement used, strength, and duration of the magnetic field [25].

In an experimental study, Ghorbani et al. [21] investigated that using magnetized water can positively affect concrete mixtures, especially its effects on foam stability, compressive strength, tensile strength, water absorption, and microstructure of foam concrete. Tests conducted on 9 different mixtures prepared with water passed through a constant magnetic field at various flow rates and in different numbers showed that using magnetized water increases foam stability and improves foam concrete's compressive and tensile strength. However, a slight decrease in the water absorption of the hardened foam concrete was observed. The high compressive strength of samples with magnetized water can be attributed to the high specific field compared to normal water. The activity of magnetized water increases, and the interaction with cement particles increases, which can increase the compressive strength and split tensile strength. Su et al. [22] have investigated the compressive strength and workability of mortar and concrete mixed with magnetic water. The study reveals a 9–19% increase in compressive strength for mortar samples using 0.8–1.35 T magnetic water and a 10–23% increase for concrete samples. Additionally, magnetic water has improved the mortar and concrete's flowability, slump, and hydration degree.

Keshta et al. [23] examined the impact of magnetized water on the compressive strength of concrete. The results indicate that the use of magnetized water increased the pH value. The magnetic field was determined to raise pH by 12.6%, possibly due to a decrease in hydrogen ion concentration. Additionally, the polarization of water molecules and a reduction in hydrogen ions enhance the organization of water molecules, improving the hydration process. This results in greater cohesive forces applied to cement-based material particles, enhancing concrete properties. The post-use increase in pH due to magnetized water reduces corrosion rates and increases compressive strength. Acidic water negatively affects concrete's compressive strength. From a workability perspective, a higher pH positively influences concrete workability; using magnetized water can reduce slump values by causing minimal excess cement and fine particles. Therefore, increasing the pH value of the water used can improve concrete properties.

3.2. Flexural Strength of GRC Composites

The flexural strengths of GRC concrete samples produced with magnetic water appear to be higher than the reference sample (Fig. 4). The direct relationship between the number of magnetic fields and the magnetic effect of water on homogeneous hydration in the flexural strength tests has been observed. In the early-age flexural strengths, the GRC concrete sample produced with water exposed to 8 magnetic fields exhibited a flexural strength trend of 18.3% compared to the reference sample in 7-day specimens. However, despite an increase in the 14-day strengths, it demonstrated an 11.4% lower performance than the reference sample. Similar to other tests, magnetic water tends to enhance the strength properties of the sample at early ages. Although the strength property of the same sample increased compared to the reference after 28 days, there

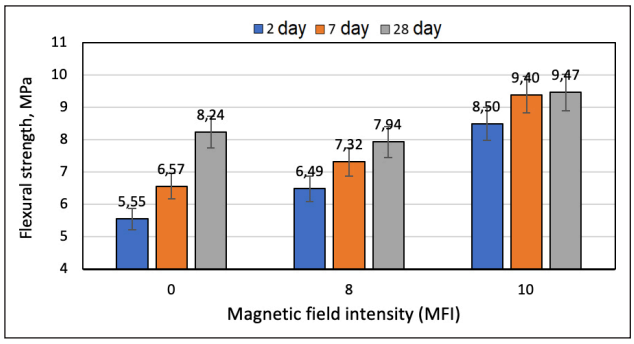

Figure 4. Flexural strengths of GRC composites produced with different magnetic waters.

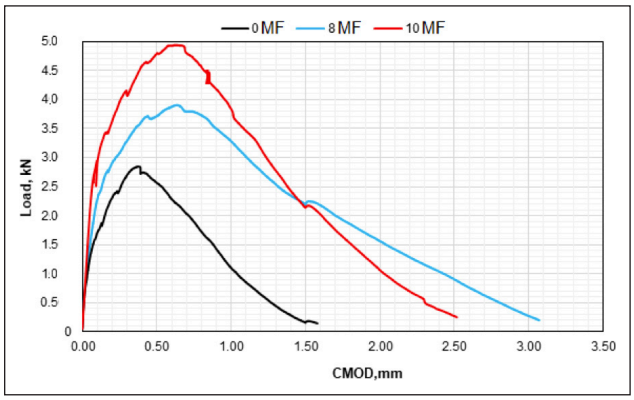

Figure 5. Fracture mechanics curves of GRC beams produced with different magnetic waters.

was a 3.64% increase in the reference sample. In GRC samples produced with water exposed to 10 magnetic fields, an increase in sound conductivity was observed, with higher percentages of 53.1%, 43.1%, and 14.9% in 7, 14, and 28-day curing times, respectively, demonstrating a tendency for a decrease in increase proportional to the curing periods compared to the reference sample.

Using magnetized water can cause cement particles to interact more strongly with water molecules. This may contribute to the cement matrix creating a stronger structure and increasing its bending strength. Also, the positive effects of magnetized water on the flexural strength of cement can be attributed to the C-S-H development in the cement paste. There is no definitive information about how magnetized water affects the C-S-H (calcium silicate hydrate) gel of cement because there are very few scientific studies on this subject. However, some research suggests that magnetized water organizes water molecules, changing the molecular structure of water, and these changes may impact cement hydration [26–28]. Cement hydration involves the formation of C-S-H gel due to the reaction of cement particles with water [29]. It is thought that using magnetized water may contribute to water molecules binding more effectively to cement particles and creating a more ordered structure in the process [30]. This may lead to the forming of a more solid and ordered structure of the C-S-H gel.

In addition to the effect of magnetized water, which is the primary purpose of this study, the most crucial factor affecting flexural strength is the glass fiber used in the mixtures. Glass fibers improve the flexural strength of cementitious composites by increasing their tensile strength. This ensures that the structural elements have a greater load-carrying capacity [31]. Glass fibers can limit the formation of cracks in concrete. This prevents cracks from propagating and ensures more consistent performance of the material [32]. Glass fibers can help make concrete more resistant to environmental influences (for example, freeze-thaw cycles), thus ensuring the longevity of the material [33]. Glass fibers can provide better shaping of the concrete mixture. This will be advantageous in accommodating bending and tensile loads, especially for architectural elements with complex or fine details [34]. In glass fiber reinforced concretes, the interaction of glass fiber with C-S-H gel during the hydration process with cement plays an important role [35]. Glass fibers can form a network surrounding the C-S-H gel, which can reduce crack formation [36]. Additionally, the surface properties of glass fibers enable hydration products to bind and form a strong bond. This interaction can increase the durability and mechanical properties of glass fiber-reinforced concrete, significantly improving tensile strength and crack resistance [37].

3.3. Fracture Mechanics of GRC Composites

Within the scope of fracture mechanics, the amount of energy absorbed by cementitious materials against fracture is examined through the three-point bending test. This test method creates a notch (crack) at one-third of the beam cross-sectional height in the middle of pre-cast cementitious beam specimens. Notched specimens are subjected to loading until a fracture occurs [38]. This test can usually be controlled by increased crack mouth opening displacement (CMOD). The load-CMOD curves of GRC concrete samples obtained using water exposed to two different numbers of magnetic fields are given in Figure 5. Considering the load values in the graph, and it is observed that the maximum fracture load increases with the increase in the number of MF. The maximum fracture load of GRC produced with water passed through NMF 8 increased by 39% compared to the reference, while the maximum fracture load of GRC produced with water passed through NMF 10 increased by 75% compared to the reference.

On the other hand, the magnetic field also positively affected the samples' flexibility. Crack opening corresponding to maximum load values was measured as 0.4, 0.62, and 0.66 mm for samples with NMF numbers of 0, 8, and 10, respectively. Also, the increase in total CMOD values proves magnetized water's positive effect on the samples' elastic properties. The positive effect of magnetized water on fracture mechanics can be attributed to the C-S-H development and the compressive and bending strength results. In addition, since the most important factor affecting the fracture mechanics of fibrous concrete is the shape of the fibers, it can be said that magnetized water also causes the homogeneous distribution of the fibers.

Aligning steel fibers is an effective way to improve the mechanical properties of steel fiber cement composites

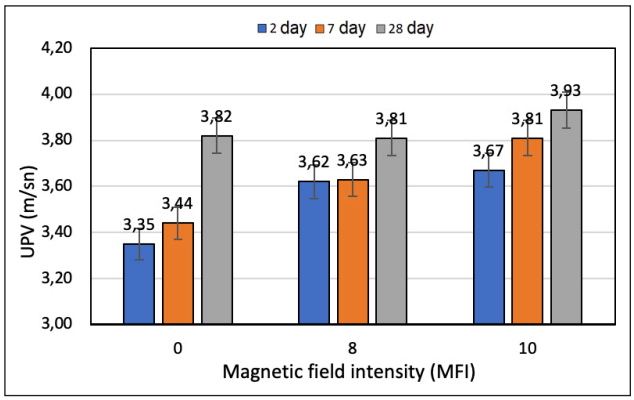

Figure 6. UPV results of GRC composites produced using water with different magnetic properties.

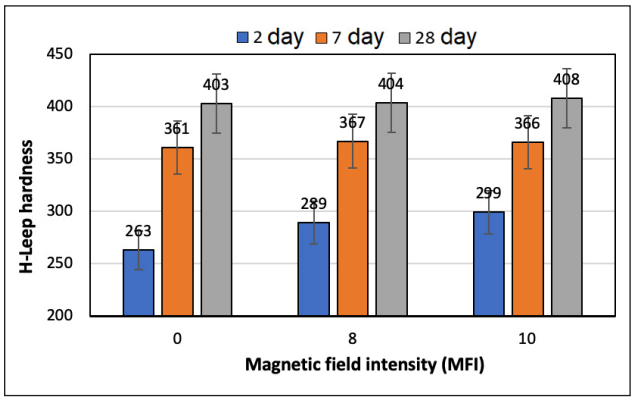

Figure 7. Effect of water exposed to different magnetic fields on H-Leep hardness values of GRC composites.

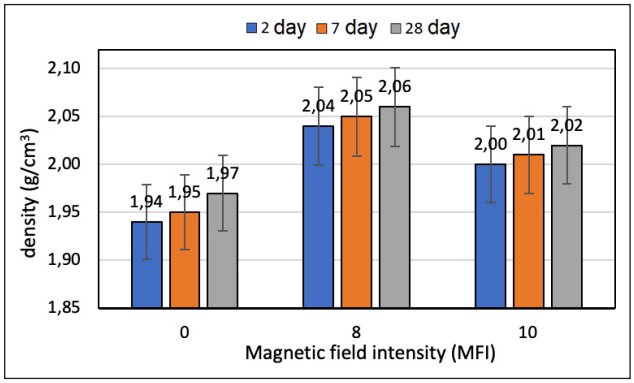

Figure 8. Density values of GRC composites produced using water with different magnetic properties.

(SFRC). Some studies have investigated creating a magnetized field to align the fibers in steel fiber-reinforced concrete. However, no specific research has been found regarding creating a magnetized field in synthetic fiber-reinforced cementitious materials or the mechanical behavior of cementitious products produced with magnetized water. Khan et al. [39] investigated the preparation and fracture behavior of aligned hooked-end steel fiber cement-based composites (ASFRC) using the magnetic field method. The mixture's rheology and the magnetic induction of the electromagnetic field for aligning steel fibers were theoretically analyzed. The results demonstrated that the cracking load and ultimate load of ASFRC increased by approximately 24–55% and 51–86%, respectively, compared to SFRC. The tensile strength and residual flexural strength of ASFRC increased by 105% and 100%, respectively. ASFRC exhibited 56–70% higher fracture energy than SFRC, indicating that the reinforcing effect of hooked-end steel fibers was superior to straight steel fibers.

3.4. UPV Test Results of GRCs

The most common method for assessing the strength quality of concrete is the compressive strength test. Alternatively, the ultrasonic pulse velocity (UPV) test can be applied as a non-destructive method to obtain information about the durability of concrete [40]. Figure 6 presents the UPV test results for GRC concretes produced with magnetized water. The GRC matrix provides sound insulation within the structure, consequently reducing the transmission speed of sound waves. The increased sound speed indicates the composite has a homogeneous and solid structure. An increase in the speed of sound indicates that the composite is in a homogeneous and robust state. The voids within the structure change inversely with density. For GRC composites produced with water exposed to 8 magnetic fields, the sound wave transmission ratios on the early ages of the 2nd and 7th days have increased by 8.06% and 5.52%, respectively, compared to the reference sample. In the GRC composites produced with water exposed to 10 magnetic fields, the speed of sound has increased by 9.55% and 10.7%, respectively. It can be inferred that water with a higher MFI number has facilitated the formation of a more homogeneous structure with lower surface tension in the cement-based composite, resulting in a structure with more voids. Therefore, sound transmission has been accelerated in the early stages due to the rapid transmission of magnetic water. In the later stage of aging, on the 28th day, the sound transmission speed of the concrete produced with magnetic water exposed to 8 magnetic fields was observed to be 0.26% less than the reference sample. However, the sound transmission speed of the GRC sample produced with water magnetized by 10 magnetic fields continued to increase by 2.88% compared to the reference sample. The increase in MFI has ensured a more homogeneous hydration reaction between cement and water in the GRC matrix, maintaining the magnetic effect of water for a more extended period and resulting in a structure with fewer voids.

When UPV values are compared with density values in terms of the use of magnetized water and regular water, it is evident that there is a parallel relationship between them. However, both UPV and density values did not yield significantly different results using magnetized water. In their experimental study, Yousry et al. [41] investigated the mechanical properties and UPV values of cement-based mortar using magnetic water. According to the results obtained, while there were profound differences between the strength values, the UPV results did not show a trend that could be followed or trusted. UPV values are generally inversely proportional to the void ratio within the material. Gaps make it

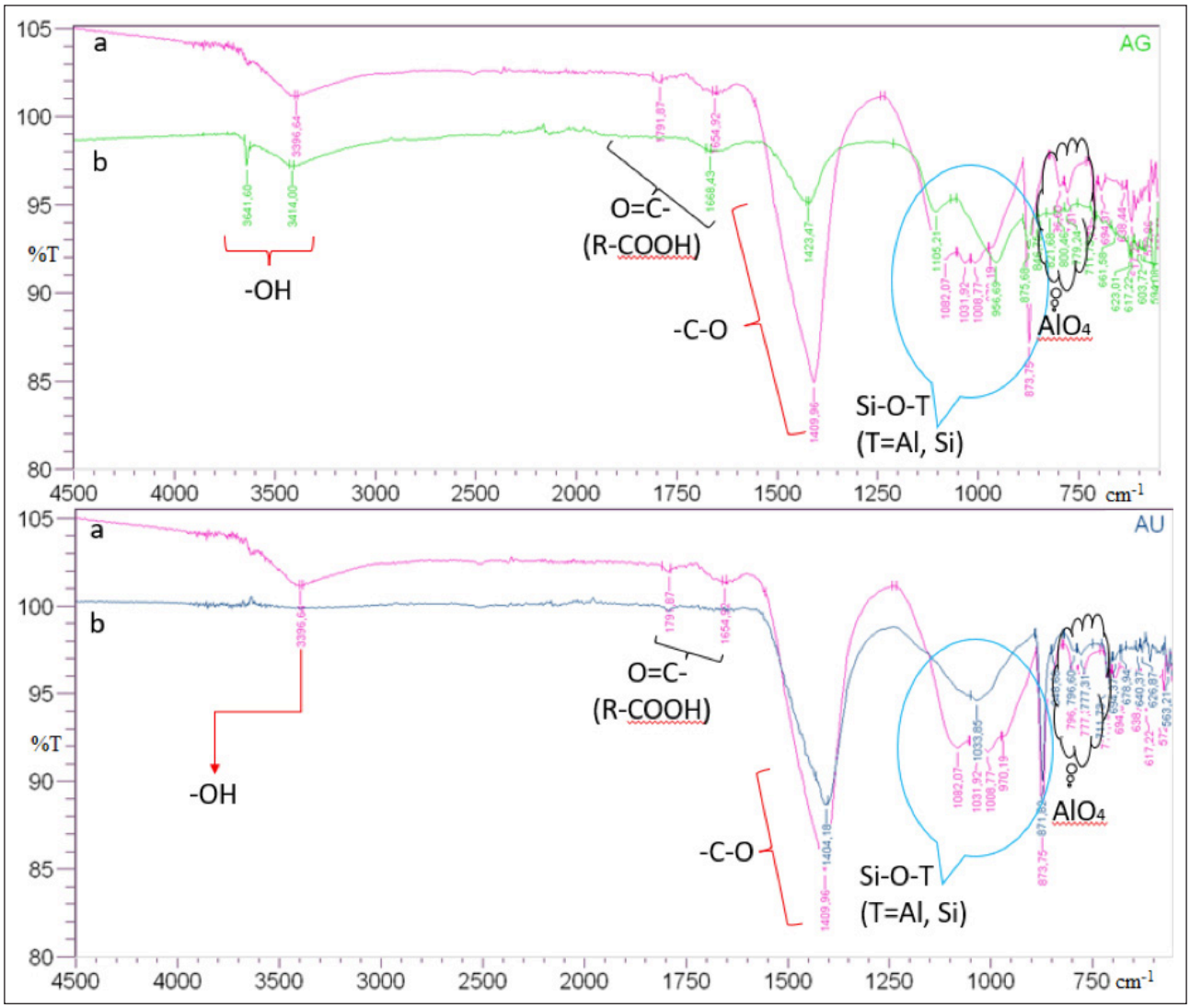

Figure 9. FTIR spectra of GRC composites produced with different magnetic waters.

difficult for sound waves to propagate, resulting in low UPV values, and a cement mat hasvoid ratio will generally have higher UPV values [42]. UPV values are directly proportional to the density of the material. A dense material allows sound waves to be transmitted more quickly and effectively, leading to high UPV values [43].

3.5. H-Leep Hardness Tests of GRC Compo

Hardness tests are a type ofprovidetructive testing that provides information about the surface hardness of cement-based structural composite materials [44]. Figure 7 shows the effects of magnetic field and curing times on Leep hardness values. The increase in curing periods has resulted in a proportional increase in hardness values for reference and other magnetized specimens. The rise in MFI has facilitated faster initial increases in Leeb values compared to the reference, with lower contribution rates throughout the curing period. The increase in the specimen left for 2 days under exposure to 8 magnetic fields is observed to be 9.88%, while for the specimen exposed to 10 magnetic fields, this ratio is 13.6%. After a curing period of 7 days, a decrease in percentage increases in Leeb values is evident, with rates of 1.66% and 1.38% for samples exposed to 8 and 10 magnetic fields, respectively. For specimens with a curing period of 28 days, the increases in Leeb hardness values are 0.24% and 1.24%, respectively. According to these values, it is observed that the magnetic water accelerates early curing periods in H-Leeb values; however, as the curing period increases, this effect diminishes.

The Schmidt hammer is the most commonly used testing tool to estimate the compressive strength of concrete non-destructively. However, few studies are in the literature on applying the Leeb hardness test to estimate concrete strength. The Leeb rebound hammer is a dynamic hardness test method and instrument developed initially for testing metallic materials. On the other hand, the Schmidt rebound hammer showed different correlations with compressive strength for concretes with different w/c ratios. The authors also discussed factors influencing the hardness value, such as surface moisture conditions and concrete carbonation. They observed that the Leeb rebound numbers were higher for older concretes and weaker concrete compositions at higher w/c ratios due to faster carbonation rates in more porous systems.

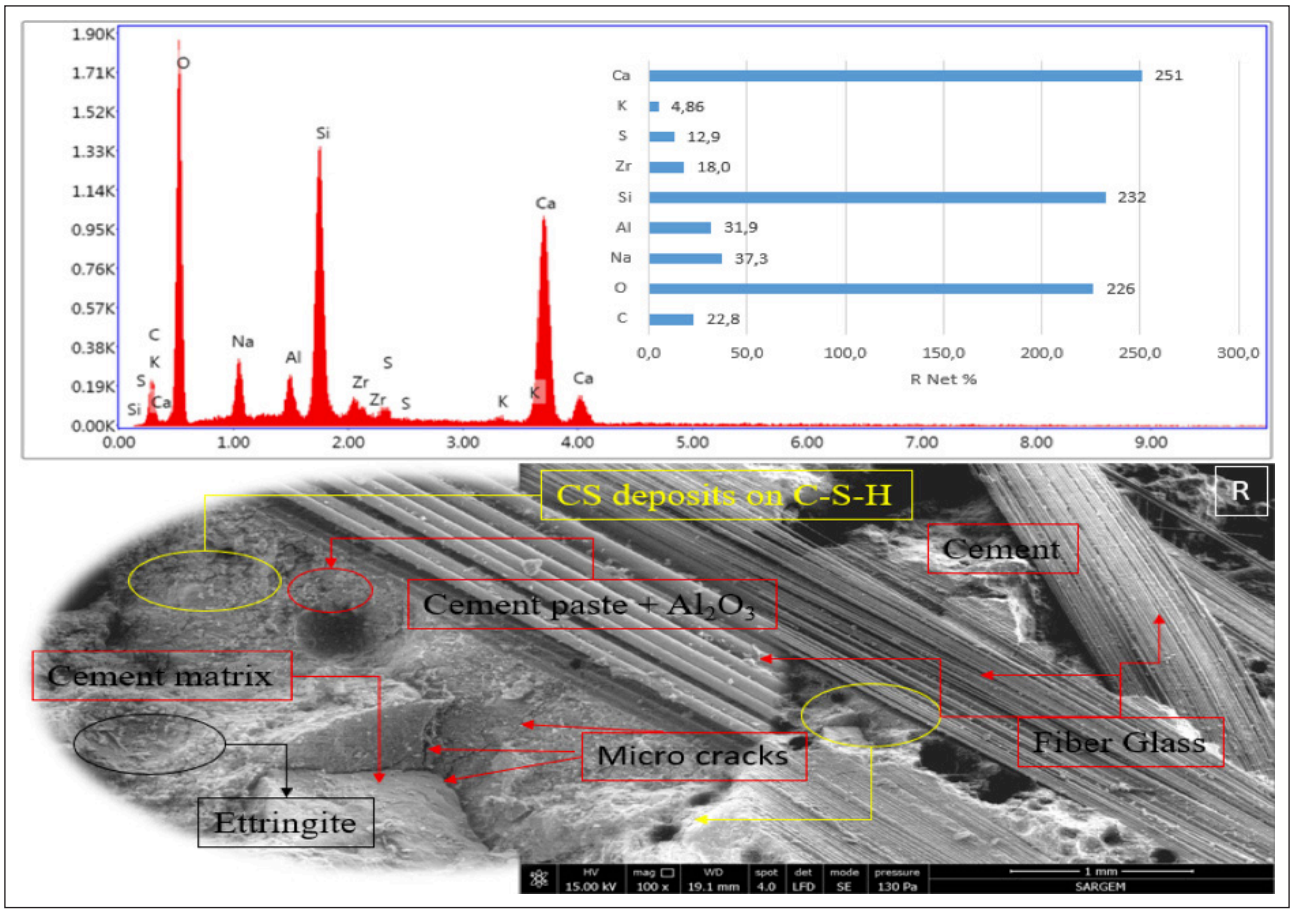

Figure 10. SEM image and EDS spectrum of reference GRC composite.

Dehghanpour et al. [38] examined the hardness properties of Ultra High Strength Concrete (UHPC) structural elements produced for facade elements. The results of the Leeb and Schmidt hammer hardness of PVA, GF, and SF-reinforced UHPC samples were compared and evaluated. A linear relationship was observed between Leeb and Rebound number values for all mixtures, and it was stated that these two hardness test methods were used to verify the values obtained from each other. While Leeb hardness values decreased in samples with PVA added, a decrease was observed in samples with GF added; There was an increase and decrease in samples with SF added. Similar changes were detected in Schmidt hardness values. The results showed that SF-reinforced samples had the highest hardness values. Compared with the literature, it was concluded that the hardness values obtained were suitable for high-strength concretes.

3.6. Density Values of GRC Composites

Before compressive strength evaluations, density measurements of GRC samples were made. The values are summarized in Figure 8. By the Archimedes principle, and these measurements explored the variations in the density values of GRC samples subjected to curing periods of 2, 7, and 28 days, as well as exposure to two different magnetic drinks of water, one at 8 and the other at 10 magnetic fields. Density differences were observed within the specified curing periods for reference samples, ranging between 1.94 and 1.97 g/cm^3. Samples produced with water obtained from 8 magnetic fields exhibited density values between 2.04–2.06 g/cm^3, while those made with water passing through 10 magnetic fields showed a distribution between 2.01–2.07 g/cm^3. In cement-based materials, density values are correlated with the water-to-binder ratio, where the binder component is typically cement [45]. In this study, as the water-to-cement ratio was kept constant, the variations in density values were found to be dependent on both the age of the concrete and the magnetic field.

The variation in density values of GRC concrete samples is generally directly associated with the curing period. The interaction of water in the mortar with cement hydration and water's subsequent evaporation from porous structures significantly influences density [46]. The magnetized water ratio resulted in a decrease in density increase compared to the reference sample, with a reduction of 5.07% on the 2nd day, 4.87% on the 7th day, and 4.83% on the 28th day. In other words, the magnetized water may have acted as a catalyst, accelerating the early curing period but losing its magnetic effect relatively quickly.

3.7. FTIR Analysis Results

FT-IR (Fourier Transform Infrared) analysis in cementitious composites is a technique used to understand the material's chemical composition and molecular structure [47]. Since polymer binders are frequently used, especial-

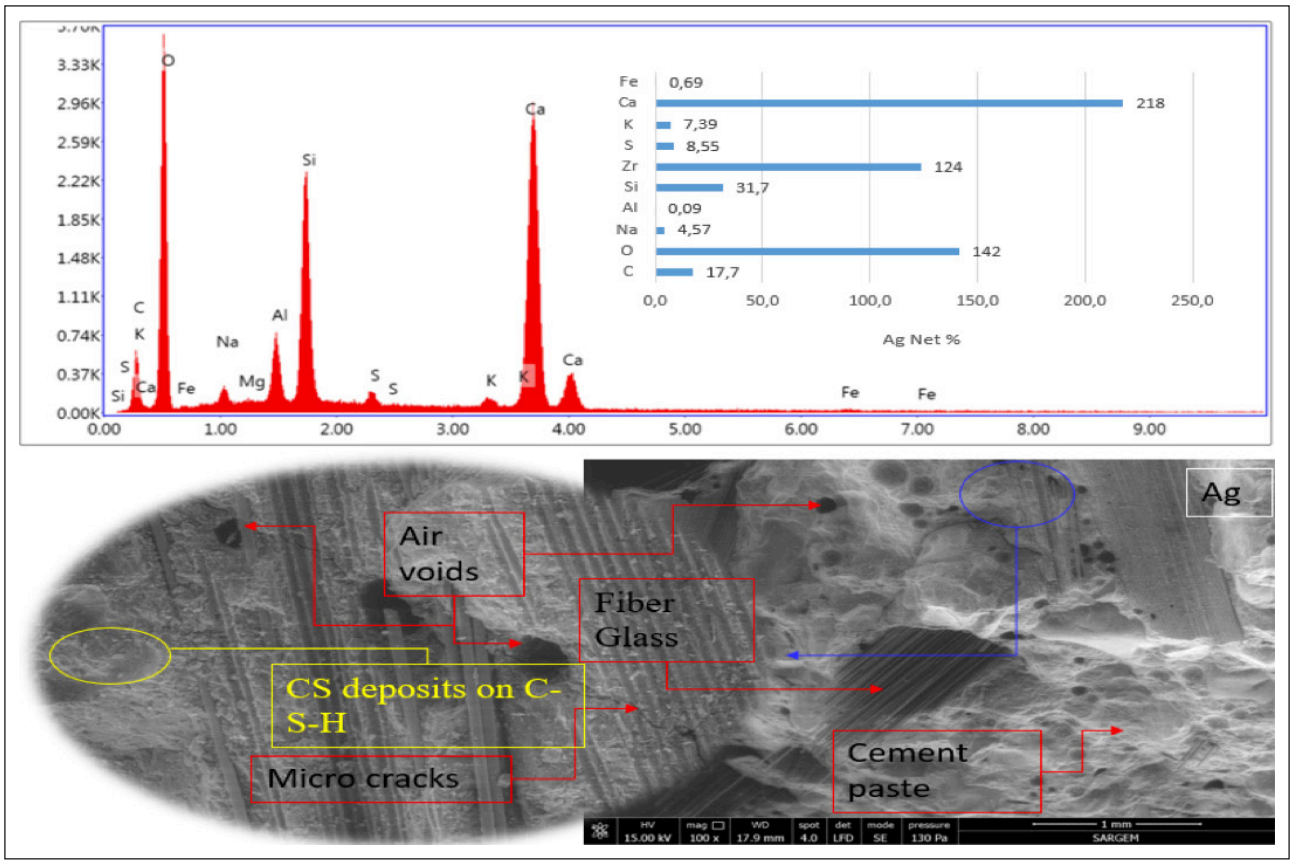

Figure 11. SEM image and EDS spectrum of GRC composite produced with water magnetized in eight magnetic fields.

ly in cementitious composites, this analysis can effectively determine the polymer's type and molecular structure. Because cementitious composites react with water during the hardening process, FT-IR analysis provides information on water content and hydration products [48]. This can affect the durability and structural properties of the material. FT-IR spectrum can identify various chemical bonds and functional groups. This gives information about the polymer material and additives or other ingredients within the composite material [49]. Cementitious composites often contain mineral additives. FT-IR analysis can help determine the presence and amount of mineral inclusions (e.g., quartz, calcite). FT-IR analysis can monitor chemical changes when cementitious composites are subjected to aging, environmental influences, or chemical attack [50].

FTIR spectra of GRC samples produced with magnetized water are given in Figure 9. The absorption bands observed at 3341.60 cm^{-1} and 3414.00 cm^{-1} in the spectrum with a magnetic field strength of 8 (Ag) are attributed to the vibrations of hydroxyl (-O-H) bonds in water molecules. These bands are also present at 3396.64 cm^{-1} in the reference spectrum. No hydroxyl band is observed in the spectrum with a magnetic field strength of 10 (Au). Previous studies [51, 52] have suggested that this band is associated with water molecules absorbed in voids formed on the surface or during copolymerization.

The bands around 1400 cm^{-1} are attributed to carbonate groups (O-C-O) formed due to the atmosphere's reaction between alkali metal hydroxides and carbon dioxide [47, 49]. The irregular strains associated with the (Si-O-X) bond encompass all vibrations around 1050 cm^{-1}. X represents silicon (Si) and aluminum (Al) atoms in a tetrahedral structure. The (Si-O-X) bond supports the geopolymerization process with the phases of the formed amorphous aluminosilicates. Studies indicate that the sharp absorption band is related to the number of tetrahedrally coordinated aluminum in the geopolymer gel [53, 54]. Peaks between 750 cm^{-1} and 800 cm^{-1} are attributed to vibrations from AlO4, while strong tension and vibration peaks between 950 cm^{-1} and 1050 cm^{-1} belong to Si-O-T (T= Al, Si). AlO4 represents a chemical group in which aluminum forms a tetrahedral structure with four oxygen atoms [55]. This may be due to amorphous aluminosilicate phases present in the cementitious composite, and these peaks provide information about the aluminum content of the material. Si-O-T represents tetrahedral structures formed by silicon bonding with oxygen and other elements [56]. These peaks offer information about the bonding pattern of silicon and aluminum in the cementitious composite.

3.8. Characterization of SEM and EDS Analysis

The Figure 10, Figure 11, and Figure 12, respectively, describe the physicochemical changes in the structure of the reference GRC sample and GRC concrete produced with water exposed to eight and ten magnetic fields, illustrating alterations during the hydration process. It has been observed that water exposure to a magnetic field leads to an increase in conductivity and a decrease in surface tension. This indi-

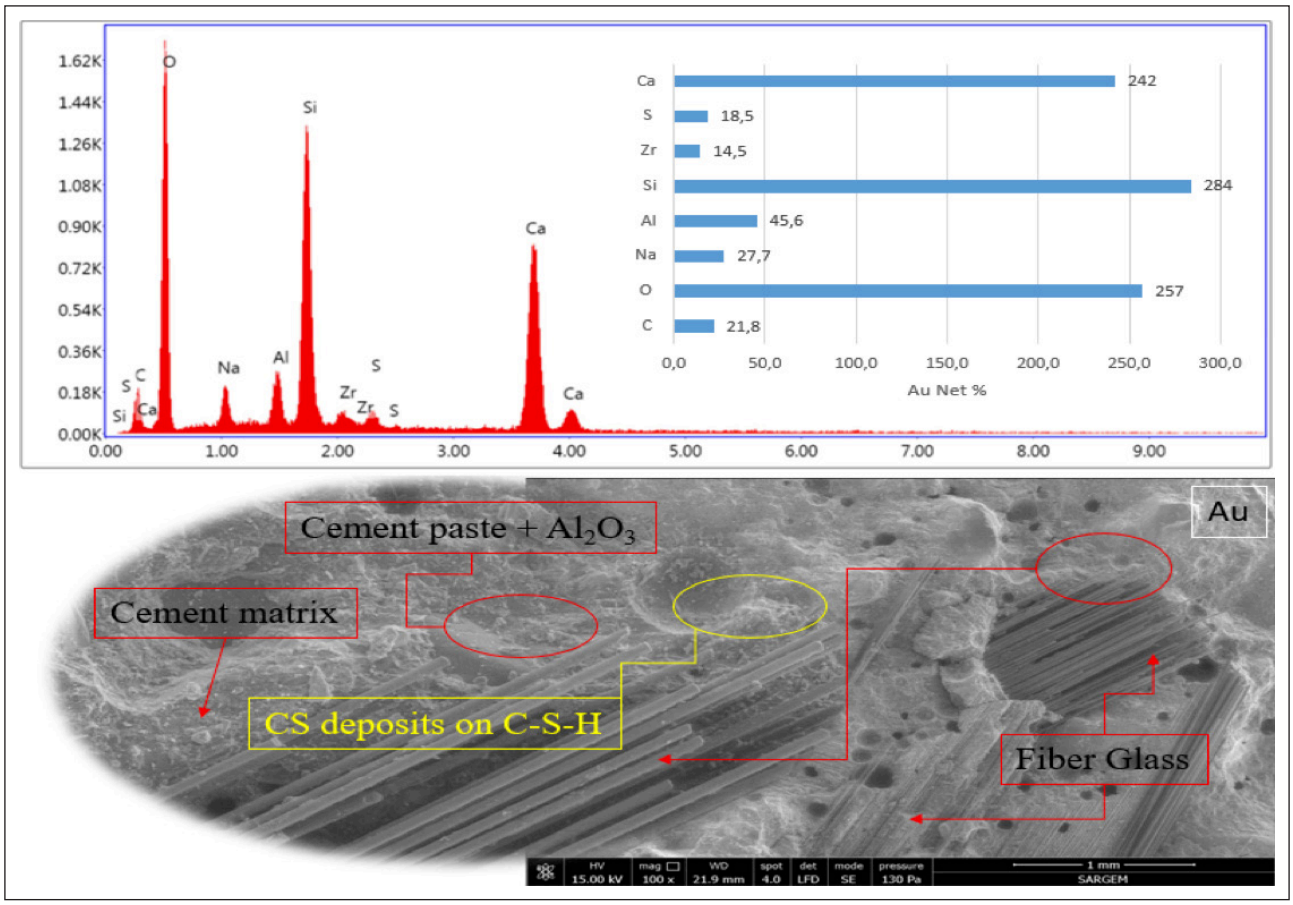

Figure 12. SEM image and EDS spectrum of GRC composite produced with water magnetized in ten magnetic fields.

cates the influence of the magnetic field on the structure of water molecules. Following exposure to the magnetic field, water molecules exhibit changes in their bonding angles, decreasing from 104.5° to 103° and forming single or more minor groups rather than clusters. The reduced surface tension allows for more homogeneous water hydration with cement, reducing the required water-to-cement ratio for setting. The quality and type of raw materials used determine the physicochemical and mechanical properties of the concrete.

Additionally, the quality and quantity of water play a significant role in determining the strength of the concrete. In the literature, although detailed explanations of how magnetic fields affect the structure of water are not explicitly mentioned, it is observed that magnetized water disperses cement particles more effectively compared to regular water. Regarding the hydration of cement, the net percentages of Ca, Al, and O elements, allowing for interpretations, have been measured as 251%, 31.9%, and 226%, respectively (Fig. 10).

According to the results of Energy Dispersive Spectroscopy (EDS) in Figure 11, the chemical element contents of the examined samples have been considered. In comparison to the reference sample, the GRC sample exposed to a magnetic field shows the presence of 218% calcium (Ca), 0.09% aluminum (Al), and 142% carbon (C) elements. This indicates a decrease in these elements compared to the reference sample. Similarly, in the EDS spectrum of the GRC sample produced with water passed through 10 identical magnetic fields (Fig. 12), 242% calcium (Ca), 45.6% aluminum (Al), and 257% oxygen (O) elements were detected. In other words, the increase in the number of magnetic fields has led to an overall increase in the percentage of aluminum, carbon, and oxygen elements. These results demonstrate that the magnetic field influences the chemical composition of GRC samples produced with water, causing significant changes in element contents.

The microstructure of cement mortar produced with water exposed to a magnetic field can be examined using various analytical techniques. Electron microscopes, X-ray scanning microscopes, and other relevant methods can be employed to assess the microstructural properties of the mortar. Water exposed to a magnetic field can influence the crystal structures of the cement mortar [57]. This can lead to changes in the crystal sizes, shapes, and distributions of cement mineral phases. The impact of the magnetic field on the water's structure can affect the porosity of the cement mortar. Achieving a more regular microstructure or reducing porosity can enhance the material's durability. Water exposed to a magnetic field can also influence the hydration process of the cement mortar, leading to the formation of different hydration products [26]. This can impact the mechanical properties of the material. This type of water can affect the homogeneous distribution of minerals in the cement mortar. This condition can determine whether the material has homogeneous mechanical properties.

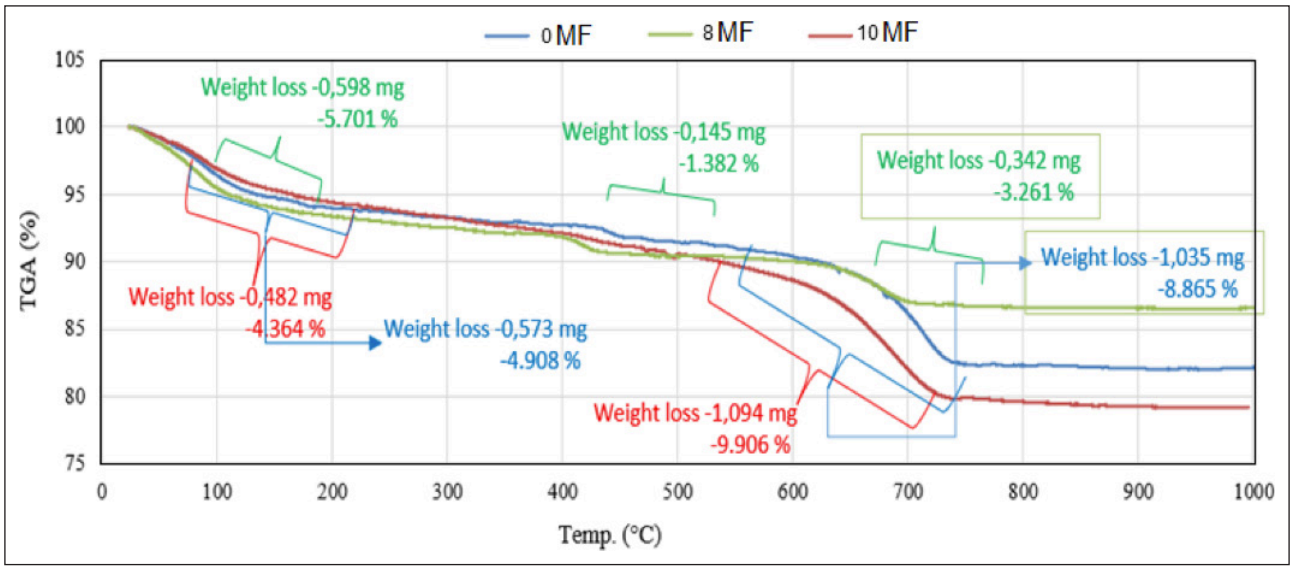

Figure 13. TGA spectrum curves of GRC composites produced with different magnetic waters.

3.9. TGA Analysis

Figure 13 shows the TGA analysis spectra of GRC samples prepared using water exposed to different numbers of magnetic fields. The amount of C-S-H increases with hydration and reaches its maximum level during heating. It is possible to predict the amount of C-S-H by measuring the water loss from C-S-H through TGA analysis. This is because the dehydration and decomposition of C-S-H and Aft (trisulfoaluminate-4CaO.3Al_2O_3.3$_2H_2O$) phases occur between 25 °C and 200 °C. However, the exact decomposition temperature of C-H-S, i.e., the range of departure of physically and chemically bound water content, is unknown. For instance, Taylor and colleagues have determined this range as 115–125 °C, while Odelson and his group have predicted a 200–400 °C range for water loss in C-S-H [58]. The water mass loss observed at 26.98–90.29 °C in the reference sample is 0.573 mg, accounting for 4.908%. For sample b with a magnetic field number (NMF) of 8, the mass loss is measured as 0.598 mg at 83.98 °C–269.0 °C, corresponding to 5.701%. In sample c with NMF = 10, the amount of lost water mass is determined as 0.482 mg at 30.01 °C–86.44 °C, accounting for 4.364%. The sample obtained with magnetic water and an NMF of 8 shows that the hydration amount is higher compared to the reference. This is because the lost water amount is directly proportional to the amount of C-S-H. Compared to the reference sample, a higher cement hydration of 4.36% is observed. The increase in the number of magnetic fields is evident in the TGA graph of sample c, showing a more precise water mass loss. The lost water amount measured as 0.482 mg in sample C, produced with water passed through 10 magnetic fields, is 15.9% higher than the reference sample.

It occurs between 105–130 °C. Some researchers say this limit can be close to 100 °C or 145 °C [59]. A similar explanation has been expressed for analyzing reactive powder concrete [60]. The amount of bound water in reactive powder concrete can be related to cement hydration through the classical Powers equation (1).

$$\propto\% = Wne(t).Wne(t\infty)*100 \quad (1)$$

Here, Wne(t) represents the amount of bound water at time t, and Wne(t∞) is the required amount of water for complete cement hydration according to the calculation by Czernin [61]. In this study, Wne(t∞) is determined to be 0.25. Thermogravimetry can also be used to predict the pozzolanic reaction of silica fume. The content of calcium hydroxide ($Ca(OH)_2$) can be calculated from the peaks observed in the DTG curve between 400 °C and 500 °C. The peak between 500 °C and 750 °C represents the decarbonization of $CaCO_3$. The decarbonization of calcium carbonate was found to be 1.035 mg with 8.865% in sample (a), 0.342 mg with 3.261% in sample (b), and 1.094 mg with 9.906% in sample (c). An increase in the amount of calcium carbonate is observed proportionally with magnetized water. Between 105 °C and 1000 °C, the dehydration and decomposition of C-S-H gel, C-H, and other hydrated products occur as water loss [62–64].

4. CONCLUSION

This study examined the changes in the physical and mechanical properties of GRC (Glass Fiber Reinforced Concrete) specimens produced with magnetic water obtained by exposing them to 8 and 10 different numbers of magnetic fields. According to the data, the H-Leep hardness value increased proportionally with the curing time. The increase in the number of magnetic fields resulted in a 9.88% and 13.6% increase in H-Leep values during 2-day intervals, 1.66% and 1.38% during 7-day curing, and 0.24% and 1.24% during 28-day curing.

While the density values of GRC specimens increased with curing periods, a decrease in density values over time was observed in specimens prepared using magnetic water. It was determined that magnetic waters reduced the air voids in the composite structure, leading to an increase in sound transmission speeds. In samples produced with magnetic water, an increase of 8.06% and 5.52% on the 2nd and 7th days, respectively,

was observed with 8 magnetic fields, and with 10 magnetic fields, these increase rates reached 9.55% and 10.7%.

In bending strength tests, a proportional increase with the curing period was observed in all GRC samples. Magnetic water increased the bending strengths of GRC samples by 18.3%, 11.4%, and 3.64% during the 7, 14, and 28 days of curing, respectively. The impact of magnetic water on compressive strength resulted in a 12.4% and 14.9% increase in the early stages and a 2.48% increase at the end of the 28 days.

In fracture mechanics analysis, a sample magnetized with 8 magnetic fields reduced the fracture strength of the GRC concrete beam by 37.1%, while increasing the number of magnetic fields by 20% resulted in a 26.5% improvement in fracture strength. In FTIR analysis, a 20% increase in magnetic fields did not show hydroxyl (-OH) and carboxyl peaks (R-COOH). SEM-EDS analysis revealed that the increase in the number of magnetic fields caused an increase in the percentages of Ca, Al, and O elements. TGA analysis indicated that a 20% increase in the magnetic field increased the amount of lost water, thereby enhancing cement hydration.

In conclusion, positive results were achieved in the physical and mechanical properties of GRC specimens produced with magnetized water. The primary reasons for this positive effect are the reduction of surface tension in magnetized water and its contribution to better hydrolysis with cement, resulting in a more homogeneous composite structure. In future studies, the effects of magnetized water on different cement composites can be investigated in more detail. This study can contribute significantly to energy savings and reduced production costs, especially considering global issues related to the efficient use of energy resources.

ACKNOWLEDGEMENTS

This study was carried out in Fibrobeton R&D Center Laboratory. We are grateful to Fibrobeton company for their support.

ETHICS

There are no ethical issues with the publication of this manuscript.

DATA AVAILABILITY STATEMENT

The authors confirm that the data that supports the findings of this study are available within the article. Raw data that support the finding of this study are available from the corresponding author, upon reasonable request.

CONFLICT OF INTEREST

The authors declare that they have no conflict of interest.

FINANCIAL DISCLOSURE

The authors declared that this study has received no financial support.

USE OF AI FOR WRITING ASSISTANCE

Not declared.

PEER-REVIEW

Externally peer-reviewed.

REFERENCES

[1] Kim, K., & Milstein, F. (1987). Relation between hardness and compressive strength of polymer concrete. *Constr Build Mater, 1*(4), 209–214. [CrossRef]

[2] Chandramouli, K., Rao, P. S. R., Narayanan, P., Tirumala, S. S., & Sravana, P. (2010). Strength properties of glass fiber concrete. *ARPN J Eng Appl Sci*, 5, 1–6.

[3] Bartos, P. J. M. (2017). Glassfibre reinforced concrete: A review. *IOP Conf Ser Mater Sci Eng, 246*, 012002. [CrossRef]

[4] Lalinde, L. F., Mellado, A., Borrachero, M. V., Monzó, J., & Payá, J. (2022). Durability of glass fiber reinforced cement (GRC) containing a high proportion of pozzolans. *Appl Sci, 12*(7), 3696. [CrossRef]

[5] Karimipour, A., Ghalehnovi, M., & de Brito, J. (2020). Mechanical and durability properties of steel fibre-reinforced rubberised concrete. *Constr Build Mater, 257*, 119463. [CrossRef]

[6] Babaloo, F., Majd, A., Arbabian, S., Sharifnia, F., & Ghanati, F. (2018). The effect of magnetized water on some characteristics of growth and chemical constituent in rice (Oryza sativa L.)Var Hashemi. *EurAsian J Biosci, 12*, 129–137.

[7] Cai, R., Yang, H., He, J., & Zhu, W. (2009). The effects of magnetic fields on water molecular hydrogen bonds. *J Mol Struct, 938*(1–3), 15–19. [CrossRef]

[8] Inaba, H., Saitou, T., Tozaki, K., & Hayashi, H. (2004). Effect of the magnetic field on the melting transition of H2O and D2O measured by a high resolution and supersensitive differential scanning calorimeter. *J Appl Phys, 96*(11), 6127–6132. [CrossRef]

[9] Shukla, S. K., Barai, S. V., & Mehta, A. (2020). *Advances in sustainable construction materials and geotechnical engineering* (Vol. 35). Springer Singapore. [CrossRef]

[10] Kimura, T. (2003). Study of the effect of magnetic fields on polymeric materials and its application. *Polym J, 35*(11), 823–843. [CrossRef]

[11] Ahmed, H. I. (2017). Behavior of magnetic concrete incorporated with Egyptian nano alumina. *Constr Build Mater, 150*, 404–408. [CrossRef]

[12] Gholhaki, M., Kheyroddin, A., Hajforoush, M., & Kazemi, M. (2018). An investigation on the fresh and hardened properties of self-compacting concrete incorporating magnetic water with various pozzolanic materials. *Constr Build Mater, 158*, 173–180. [CrossRef]

[13] Wei, H., Wang, Y., & Luo, J. (2017). Influence of magnetic water on early-age shrinkage cracking of concrete. *Constr Build Mater, 147*, 91–100. [CrossRef]

[14] Marasli, M., Subasi, S., & Dehghanpour, H. (2022). Development of a maturity method for GFRC shell concretes with different fiber ratios. *Eur J Environ Civ Eng, 26*(10):1–19. [CrossRef]

[15] Subasi, S., Dehghanpour, H., & Marasli, M. (2022). Production and characterization of GRC-SWCNT composites for shell elements. *Mater Sci, 28*(4), 423–433. [CrossRef]

[16] TS EN 196-1. (2005). *Methods of testing cement–Part 1: Determination of strength*. Turkish Standards.
[17] ASTM A956. (2006). *Standard test method for Leeb hardness testing of steel products*. ASTM International.
[18] TS EN 1170-4. (1999). *Precast concrete products-test method for glass-fibre reinforced cement-part 4: Determination of flexural strength*. Turkish Standards.
[19] ASTM C597. (2009). *Standard test method for pulse velocity through concrete*. ASTM International.
[20] Guo, Y. Z., Yin, D. C., Cao, H. L., Shi, J. Y., Zhang, C. Y., Liu, Y. M., Huang, H. H., Liu, Y., Wang, Y., Guo, W. H., Qian, A. R. & Shang, P. (2012). Evaporation rate of water as a function of a magnetic field and field gradient. *Int J Mol Sci, 13*(12), 16916–16928. [CrossRef]
[21] Ghorbani, S., Ghorbani, S., Tao, Z., de Brito, J., & Tavakkolizadeh, M. (2019). Effect of magnetized water on foam stability and compressive strength of foam concrete. *Constr Build Mater, 197*, 280–290. [CrossRef]
[22] Su, N., Wu, Y. H., & Mar, C. Y. (2000). Effect of magnetic water on the engineering properties of concrete containing granulated blast-furnace slag. *Cem Concr Res, 30*(4), 599–605. [CrossRef]
[23] Keshta, M. M., Yousry Elshikh, M. M., Kaloop, M. R., Hu, J. W., & ELMohsen, I. A. (2022). Effect of magnetized water on characteristics of sustainable concrete using volcanic ash. *Constr Build Mater, 361*, 129640. [CrossRef]
[24] Ghorbani, S., Gholizadeh, M., & de Brito, J. (2020). Effect of magnetized mixing water on the fresh and hardened state properties of steel fibre reinforced self-compacting concrete. *Constr Build Mater, 248*, 118660. [CrossRef]
[25] Hu, H. X., & Deng, C. (2021). Effect of magnetized water on the stability and consolidation compressive strength of cement grout. *Mater Basel, 14*(2), 275. [CrossRef]
[26] Ramalingam, M., Narayanan, K., Masilamani, A., Kathirvel, P., Murali, G., & Vatin, N. I. (2022). Influence of magnetic water on concrete properties with different magnetic field exposure times. *Mater Basel, 15*(12), 4291. [CrossRef]
[27] Elkerany, A. M., Yousry Elshikh, M. M., Elshami, A. A., & Youssf, O. (2023). Effect of water magnetization technique on the properties of metakaolin-based sustainable concrete. *Constr Mater, 3*(4), 434–448. [CrossRef]
[28] Ghorbani, S., Gholizadeh, M., & de Brito, J. (2018). Effect of magnetized water on the mechanical and durability properties of concrete block pavers. *Mater Basel, 11*(9), 1647. [CrossRef]
[29] Kong, D., Huang, S., Corr, D., Yang, Y., & Shah, S. P. (2018). Whether do nano-particles act as nucleation sites for C-S-H gel growth during cement hydration? *Cem Concr Compos, 87*, 98–109. [CrossRef]
[30] Mohammadnezhad, A., Azizi, S., Sousanabadi, H. F., Tashan, J., & Habibnejad, A. K. (2022). Understanding the magnetizing process of water and its effects on cementitious materials: A critical review. *Constr Build Mater, 356*, 129076. [CrossRef]
[31] Al-Gemeel, A. N., Zhuge, Y., & Youssf, O. (2018). Use of hollow glass microspheres and hybrid fibres to improve the mechanical properties of engineered cementitious composite. *Constr Build Mater, 171*, 858–870. [CrossRef]
[32] Shafei, B., Kazemian, M., Dopko, M., & Najimi, M. (2021). State-of-the-art review of capabilities and limitations of polymer and glass fibers used for fiber-reinforced concrete. *Mater Basel, 14*(2), 409. [CrossRef]
[33] Yan, F., Lin, Z., Zhang, D., Gao, Z., & Li, M. (2017). Experimental study on bond durability of glass fiber reinforced polymer bars in concrete exposed to harsh environmental agents: Freeze-thaw cycles and alkaline-saline solution. *Compos Part B Eng, 116*, 406–421. [CrossRef]
[34] Marasli, M., Subasi, S., & Dehghanpour, H. (2022). Development of a maturity method for GFRC shell concretes with different fiber ratios. *Eur J Environ Civ Eng, 26*(10), 1–19. [CrossRef]
[35] Wu, C., He, X., Zhao, X., He, L., Song, Y., & Zhang, X. (2022). Effect of fiber content on mechanical properties and microstructural characteristics of alkali resistant glass fiber reinforced concrete. *Adv Mater Sci Eng, 2022*, 1–19. [CrossRef]
[36] Chen, H., Wang, P., Pan, J., Lawi, A. S., & Zhu, Y. (2021). Effect of alkali-resistant glass fiber and silica fume on mechanical and shrinkage properties of cement-based mortars. *Constr Build Mater, 307*, 125054. [CrossRef]
[37] Balea, A., Fuente, E., Monte, M. C., Blanco, Á., & Negro, C. (2021). Fiber reinforced cement based composites. *In Fiber reinforced composites* (pp. 597–648). Elsevier. [CrossRef]
[38] Dehghanpour, H., Subasi, S., Guntepe, S., Emiroglu, M., & Marasli, M. (2022). Investigation of fracture mechanics, physical and dynamic properties of UHPCs containing PVA, glass and steel fibers. *Constr Build Mater, 328*, 127079. [CrossRef]
[39] Khan, S., Qing, L., Ahmad, I., Mu, R., & Bi, M. (2022). Investigation on fracture behavior of cementitious composites reinforced with aligned hooked-end steel fibers. *Mater Basel, 15*(2), 542. [CrossRef]
[40] Kim, W., & Lee, T. (2023). A study to improve the reliability of high-strength concrete strength evaluation using an ultrasonic velocity method. *Mater Basel, 16*(20), 6800. [CrossRef]
[41] Yousry, O. M. M., Abdallah, M. A., Ghazy, M. F., Taman, M. H., & Kaloop, M. R. (2020). A study for improving compressive strength of cementitious mortar utilizing magnetic water. *Mater Basel, 13*(8), 1971. [CrossRef]
[42] Constantinides, G., & Ulm, F. J. (2004). The effect of two types of C-S-H on the elasticity of cement-based materials: Results from nanoindentation and micromechanical modeling. *Cem Concr Res, 34*(1), 67–80. [CrossRef]
[43] Lafhaj, Z., Goueygou, M., Djerbi, A., & Kaczmarek, M. (2006). Correlation between porosity, permeability and ultrasonic parameters of mortar with variable water/cement ratio and water content. *Cem Concr Res, 36*(4), 625–633. [CrossRef]

[44] Mishra, D. A., & Basu, A. (2013). Estimation of uniaxial compressive strength of rock materials by index tests using regression analysis and fuzzy inference system. *Eng Geol, 160*, 54–68. [CrossRef]

[45] Tassew, S. T., & Lubell, A. S. (2014). Mechanical properties of glass fiber reinforced ceramic concrete. *Constr Build Mater, 51*, 215–224. [CrossRef]

[46] Amran, Y. H. M., Farzadnia, N., & Abang Ali, A. A. (2015). Properties and applications of foamed concrete: A review. *Constr Build Mater, 101*, 990–1005. [CrossRef]

[47] Yusuf, M. O. (2023). Bond characterization in cementitious material binders using Fourier-transform infrared spectroscopy. *Appl Sci, 13*(5), 3353. [CrossRef]

[48] Sun, H., Ding, Y., Jiang, P., Wang, B., Zhang, A., & Wang, D. (2019). Study on the interaction mechanism in the hardening process of cement-asphalt mortar. *Constr Build Mater, 227*, 116663. [CrossRef]

[49] Cosentino, A. G. M., Silva, F. C., da Silva, G., Sciamareli, J., & da Costa Mattos, E. (2020). A short review about aerospace materials characterization – Bonding agents and thermal insulation. *Propellants Explos Pyrotech, 45*(8), 1175–1184. [CrossRef]

[50] Muthu, M., Yang, E. H., & Unluer, C. (2021). Effect of graphene oxide on the deterioration of cement pastes exposed to citric and sulfuric acids. *Cem Concr Compos, 124*, 104252. [CrossRef]

[51] Ng, C., Alengaram, U. J., Wong, L. S., Mo, K. H., Jumaat, M. Z., & Ramesh, S. (2018). A review on microstructural study and compressive strength of geopolymer mortar, paste and concrete. *Constr Build Mater, 186*, 550–576. [CrossRef]

[52] Caggiani, M. C., Occhipinti, R., Finocchiaro, C., Fugazzotto, M., Stroscio, A., Mazzoleni, P., & Barone, G. (2022). Diffuse reflectance infrared Fourier transform spectroscopy (DRIFTS) as a potential on site tool to test geopolymerization reaction. *Talanta, 250*, 123721. [CrossRef]

[53] Benavent, V., Steins, P., Sobrados, I., Sanz, J., Lambertin, D., Frizon, F., Rossignol, S., & Poulesquen, A. (2016). Impact of aluminum on the structure of geopolymers from the early stages to consolidated material. *Cem Concr Res, 90*, 27–35. [CrossRef]

[54] Duxson, P., Provis, J. L., Lukey, G. C., Separovic, F., & van Deventer, J. S. J. (2005). 29Si NMR study of structural ordering in aluminosilicate geopolymer gels. *Langmuir, 21*(7), 3028–3036. [CrossRef]

[55] Schroeder, R. A., & Lyons, L. L. (1966). Infra-red spectra of the crystalline inorganic aluminates. *J Inorg Nucl Chem, 28*(5), 1155–1163. [CrossRef]

[56] Qu, J., Zhang, J., Li, H., Li, S., Hou, Z., Chang, R., & Zhang, Y. (2024). Coal gasification slag-derived highly reactive silica for high modulus sodium silicate synthesis: Process and mechanism. *Chem Eng J, 479*, 147771. [CrossRef]

[57] Wang, Y., Liu, Z., He, F., Zhuo, W., Yuan, Q., Chen, C., & Yang, J. (2021). Study on water instability of magnesium potassium phosphate cement mortar based on low-field 1H nuclear magnetic resonance. *Measurement, 180*, 109523. [CrossRef]

[58] Blanc, P., Bourbon, X., Lassin, A., & Gaucher, E. C. (2010). Chemical model for cement-based materials: Temperature dependence of thermodynamic functions for nanocrystalline and crystalline C–S–H phases. *Cem Concr Res, 40*(6), 851–866. [CrossRef]

[59] Deboucha, W., Leklou, N., Khelidj, A., & Oudjit, M. N. (2017). Hydration development of mineral additives blended cement using thermogravimetric analysis (TGA): Methodology of calculating the degree of hydration. *Constr Build Mater, 146*, 687–701. [CrossRef]

[60] Kim, J. J., Foley, E. M., & Reda Taha, M. M. (2013). Nano-mechanical characterization of synthetic calcium–silicate–hydrate (C–S–H) with varying CaO/SiO2 mixture ratios. *Cem Concr Compos, 36*, 65–70. [CrossRef]

[61] Loukili, A., Khelidj, A., & Richard, P. (1999). Hydration kinetics, change of relative humidity, and autogenous shrinkage of ultra-high-strength concrete. *Cem Concr Res, 29*(4), 577–584. [CrossRef]

[62] Heikal, M. (2016). Characteristics, textural properties and fire resistance of cement pastes containing Fe2O3 nano-particles. *J Therm Anal Calorim, 126*(3), 1077–1087. [CrossRef]

[63] Saraya, M. E. S. I. (2014). Study physico-chemical properties of blended cements containing fixed amount of silica fume, blast furnace slag, basalt and limestone, a comparative study. *Constr Build Mater, 72*, 104–112. [CrossRef]

[64] Zhang, Q., & Ye, G. (2011). Microstructure analysis of heated Portland cement paste. *Procedia Eng, 14*, 830–836. [CrossRef]